Phase transitions and critical phenomena in alloys with random anisotropy

K. M. Lee and M. J. O'Shea
Department of Physics, Kansas State University, Manhattan, Kansas 66506-2601
(Received 1 April 1993; revised manuscript received 19 July 1993)

The effects of random magnetic anisotropy on ferromagnetic critical behavior in four rare-earth-based amorphous alloys, $Gd_{65}Co_{35}$, $Nd_{50}Co_{50}$, $Nd_{65}Co_{35}$, and $Tb_{65}Co_{35}$, are reported. The ratio of anisotropy to exchange, D/J_0, ranges from 0.004(1) to 0.323(35) in these alloys. The zero-field state of the anisotropic alloys (Nd and Tb based) is spin-glass-like below T_c. In order to determine the extent of the critical regime as a function of reduced temperature, $\epsilon=(T-T_c)/T_c$, and to determine if the asymptotic critical regime is probed, a wide range of ϵ is covered. Evidence for crossovers as a function of applied field and as a function of D/J_0 are observed. As a function of applied field, the alloys containing anisotropic rare-earth atoms cross over with increasing field from a state that shows the characteristics of a speromagnet to a state where the magnetic isotherms follow a ferromagnetic-scaling equation of state. The field above which good ferromagnetic scaling is observed increases monotonically with D/J_0. No deviations from scaling were found at small ϵ giving confidence that the asymptotic critical regime is probed. Deviations from scaling were seen at large values of ϵ ($\epsilon > 0.06$) which gives the limit of the critical regime. We find systematic variations in the measured ferromagnetic critical exponents γ and δ with D/J_0 indicating a crossover in critical behavior presumably from an isotropic to a random anisotropy class with increasing D/J_0. Finally, we point out that there are some theoretical hints of a ferromagneticlike state below T_c in random-anisotropy models.

I. INTRODUCTION

We report studies of critical phenomena in magnetic systems with both weak and strong random magnetic anisotropy (RMA). The Hamiltonian in its simplest form for such a system can be written[1]

$$H=-J_0\sum_{ij}\mathbf{S}_i\cdot\mathbf{S}_j-D\sum_i(\hat{\mathbf{n}}_i\cdot\mathbf{S}_i)^2\ ,$$

where J_0 is the average exchange strength, $\mathbf{S}$ represents the spin at site i or j, D is the anisotropy strength, and $\hat{\mathbf{n}}_i$ is a unit vector describing the anisotropy axis at site i. For a RMA system, $\hat{\mathbf{n}}_i$ varies in direction from site to site. Systems with strong RMA are interesting since their zero-field order is speromagnetic (or a more complex disordered state such as sperimagnetic) at low temperatures.[1-3] This state is a spin-glass-like state in which the spins, rather than being collinearly ordered, are frozen along their local anisotropy axes. A good understanding of the static properties of the low-temperature magnetic state in RMA systems has been achieved. Chudnovsky, Saslow, and Serota[4] have shown within a semiphenomenological model for the case of small anisotropy that the spins are ferromagnetically correlated over a short distance at low temperatures in zero field. This state is referred to as a correlated speromagnet and its susceptibility can be large. In small fields this model exhibits a ferromagnetic state with long-range order in which the local magnetization vector "wanders" with its average direction being along the applied field. We have shown in amorphous Er- and Tb-based alloys[5] at low temperatures ($T\cong 0.05T_c$) that this zero-field state with no long-range magnetic order is converted into a ferromagnetic state with long-range order by a small magnetic field as predicted by the above model of Ref. 4. Work has also been done at low temperatures in amorphous Dy-based systems in which a similar result is reported.[6]

The nature of the phase transition and associated critical phenomena at T_c in RMA systems is less well understood. Experimentally, it has been shown[7,8] that in RMA systems the nonlinear magnetization given by $M_{\rm NL}=M-\chi_0 H$ (χ_0 is the zero-field susceptibility) follows a spin-glass scaling[9] equation of state. More recently, it was shown by us that this scaling crosses over to a ferromagnetic scaling for sufficiently high fields (of order 1 kOe) for Tb-based systems.[10,11] Theoretically, it has been shown that for space dimensionality $d\leq 4$ and for spin components $m_s\geq 2$, no long-range order exists in zero applied field.[12,13] This has been confirmed in a number of rare-earth–transition-metal amorphous alloys by neutron-scattering measurements.[14] A calculation of the magnetic equation of state for a RMA system indicates that the susceptibility does not diverge[13] and is limited to $\chi=A(D/J_0)^{-4}$ (A is a constant) and there is experimental evidence supporting this.[15] Below T_c a number of RMA models show ferromagnetic spin correlations which decay in a power-law fashion with distance.[13,16-18] This state is referred to as a quasiferromagnetic state because of the relatively slow ferromagnetic correlation decay this power law implies. A simulated annealing calculation yields a large (but not divergent) ferromagnetic correlation length below T_c for RMA systems.[19]

Scaling theory is at the heart of the description of critical phenomena in many systems including magnetic,[20,21] liquid, and superfluid systems.[20,22,23] According to the universality principle, the critical exponents associated with scaling are determined by the spatial dimension and

the order-parameter dimension of the system. The source and strength of the ordering interaction are not important in determining the critical-exponent values. Universality has been confirmed experimentally for a number of liquid and superfluid systems and the critical exponents agree with model predictions.[22,23]

In the simple ferromagnets Fe, Co, Ni, and Gd, the measured critical exponents cover a range of values, and for Co and Gd, the critical exponents differ from those predicted by the Heisenberg model with short-range interactions.[24] In the case of transition-metal magnetic system, the most careful work indicates that the critical regime, that is, the reduced temperature below which the measured critical exponents do not vary with temperature, is given by $|\epsilon| < 0.06$. The exponent γ associated with susceptibility has been studied in some detail and shows an anomalous increase over its critical value for $\epsilon > 0.06$ for a number of amorphous transition-metal alloys.[25] Also, inclusion of data outside the critical regime in scaling analyses can result in erroneous values of the critical exponents[26] even though apparently high-quality scaling may be obtained.

In addition to the exchange interactions which produce magnetic ordering in these systems, weaker anisotropic interactions such as dipolar anisotropy[21,27] are present in all these systems, and both Co (Ref. 28) and Gd (Ref. 29) have a uniaxial (crystalline) anisotropy associated with the c axis of their hcp structure. The presence of these weaker interactions can produce crossover effects close to T_c, making it difficult to observe the asymptotic critical regime. For example, Hargraves *et al.*[30] have measured the magnetic susceptibility for crystalline Gd and find for $\epsilon > 10^{-3}$ a critical exponent γ of 1.22(2). For $\epsilon < 10^{-3}$, the data cannot be described by a simple power-law behavior, suggesting that the asymptotic critical regime has not been probed for $\epsilon > 10^{-3}$. A dipolar anisotropy mechanism was ruled out as a cause of these deviations of susceptibility from power-law behavior, but a weak uniaxial crystalline anisotropy may provide an explanation.

In this work we examine the critical phenomena including scaling at the magnetic phase transition for selected amorphous alloys which cover a range of values of D/J_0. In order of increasing D/J_0, the amorphous alloys we study are $Gd_{65}Co_{35}$, $Nd_{50}Co_{50}$, $Nd_{65}Co_{35}$, and $Tb_{65}Co_{35}$. Since these materials are amorphous, no coherent uniaxial anisotropy is present. The purpose of our studies is to (i) determine the critical exponents characterizing the magnetic phase transition and to do scaling analyses over as small a reduced temperature range as possible to check that the asymptotic critical regime is being probed and (ii) discern any dependence of the critical behavior on the RMA strength in these systems. A preliminary report of critical behavior over a limited reduced temperature range has been made for $Tb_{65}Co_{35}$.[11]

II. SAMPLE PREPARATION, STRUCTURE, AND EXPERIMENTAL TECHNIQUE

The $Gd_{65}Co_{35}$, $Nd_{65}Co_{35}$, and $Tb_{65}Co_{35}$ amorphous alloys are prepared by splat cooling and are in the form of foils about 50 μm thick and 3 cm in diameter. The amorphous $Nd_{50}Co_{50}$ alloy is somewhat more difficult to make, and melt spinning which has a slightly faster quench rate than splat cooling is used. The composition is determined from the initial weights of the component elements and checked by weighing after melting and is accurate to 0.2%. The structure of these materials is characterized by x-ray diffraction, and broad peaks characteristic of amorphous materials are found. Some examples of x-ray diffractograms are given in Refs. 5 and 31. For magnetization measurements strips 3 mm wide and 30–50 μm thick are cut from the foil and sandwiched together. The strips were aligned with their long axis parallel to the applied field to minimize demagnetization effects.

Detailed magnetization measurements up to 55 kOe were then done using a Quantum Design superconducting quantum interference device (SQUID) magnetometer. Magnetization measurements were only made if the temperature was within ± 0.01 K of the set temperature, the maximum temperature resolution available. The systematic error in the temperature measurement itself is ± 0.05 K.

III. MAGNETIC STATE AND ANISOTROPY OF RARE-EARTH AMORPHOUS ALLOYS

The strength of the RMA (D) and exchange (J_0) are determined by the magnetization-area method and from the transition temperature, respectively, as described in Ref. 5, and their ratio D/J_0 is given in Table I for the alloys of this work. We chose $Gd_{65}Co_{35}$, $Nd_{50}Co_{50}$, $Nd_{65}Co_{35}$, and $Tb_{65}Co_{35}$ to do detailed studies of critical phenomena since these alloys span a large range of D/J_0, from 0.004 to 0.323.

These systems are two-component magnetic systems since Co carries a moment. The exchange interaction between the rare-earth and transition-metal moments is antiferromagnetic for Gd (or Tb) and Co. Thus $Gd_{65}Co_{35}$ (no RMA) is ferromagnetic and exhibits a demagnetization limited susceptibility.[32] $Tb_{65}Co_{35}$ (strong RMA) is sperimagnetic, and the magnetic susceptibility exhibits a small cusp[5] similar to that seen in spin glasses. In this latter state the Tb moments align along their local anisotropy axes and the Co moments align in the opposite direction to the local average Tb moment.[33] Since the interaction between the rare-earth and transition-metal moments is ferromagnetic for Nd and Co, both of the Nd al-

TABLE I. Ratio of anisotropy to exchange strength D/J_0, and H_d the field below which deviations from scaling occur. The value of H_d for $Tb_{50}Gd_{15}Co_{35}$ is taken from Ref. 10 and data presented therein.

	D/J_0	H_d (Oe)
$Gd_{65}Co_{35}$	0.004(1)	200(50)
$Nd_{50}Co_{50}$	0.008(1)	100(50)
$Nd_{65}Co_{35}$	0.190(9)	500(50)
$Tb_{50}Gd_{15}Co_{35}$	0.222(20)	700(100)
$Tb_{65}Co_{35}$	0.323(35)	1000(100)

loys are speromagnetic. In this state the Co moment lines up with the average local Nd moment. Again, the magnetic susceptibility exhibits a cusp and an example is given for $Nd_{65}Co_{35}$ in Ref. 5. The Co moment is small ($<0.5\mu_B$) in all the alloys except $Nd_{50}Co_{50}$. Since the rare-earth moment may have additional contributions from the conduction electron polarization, it is difficult to separate out the rare-earth and transition-metal moments. In the case of $Gd_{65}Co_{35}$, a detailed study has been done and the moments have been determined to be $(7.5\pm0.1)\mu_B$ for Gd and $(0.4\pm0.2)\mu_B$ for Co.[34]

Generally, in amorphous systems there will be spatial fluctuations in the exchange. If these exchange fluctuations are strong enough, a spin-glass state is present at low temperatures. In $Gd_{65}Co_{35}$ the magnetic order is collinear, indicating that if exchange fluctuations are present, they are not strong enough to produce a spin-glass state. This suggests that the RMA incorporated by Tb or Nd is responsible for the spin disorder. A consequence of the RMA is that large coercivities (>5 kOe) are observed in alloys containing anisotropic rare-earth atoms at low temperatures.[1-3,5] Such a large coercivity is not found in alloys where the spin disordering is produced by exchange fluctuations.

A small demagnetization correction determined from an Arrott plot[21] is made to the applied field H_a to determine the internal field, $H=H_a-NM$, where N is the demagnetization factor. This correction is important for $Gd_{65}Co_{35}$, which shows a demagnetization limited susceptibility. In the other alloys of this work, the susceptibility is small and so the demagnetization correction is also small.

IV. CRITICAL BEHAVIOR

We define the critical exponents α, β, γ, and δ and the power-law coefficients B_1, m_0, h_0/m_0, and B_4 (critical amplitudes) by the equations

$$C_v=B_1|\epsilon|^{-\alpha}, \tag{1a}$$

$$M_s=m_0|\epsilon|^{\beta}, \quad \epsilon<0, \tag{1b}$$

$$\chi=(m_0/h_0)|\epsilon|^{-\gamma}, \quad \epsilon>0, \tag{1c}$$

$$M=B_4H^{1/\delta}, \quad \epsilon=0. \tag{1d}$$

C_v, M_s, χ, and M are the specific heat at constant volume, spontaneous magnetization, susceptibility, and magnetization as a function of applied field, respectively. Scaling theory[20] then gives

$$\alpha=2(1-\beta)-\gamma, \quad \gamma=\beta(\delta-1). \tag{2}$$

To determine T_c and γ, Eq. (1c) may be differentiated to give

$$X=(T-T_c)/\gamma, \quad X=1/(\chi d\chi^{-1}/dT). \tag{3}$$

A plot of X versus T will give an x-axis intercept of T_c and a slope of $1/\gamma$. Such a plot is shown for $Gd_{65}Co_{35}$ in Fig. 1(a) and the values of T_c and γ are given in Table II. A double-logarithmic plot of the critical isotherm ($T=T_c$), shown in Fig. 1(b), is then used to determine δ for $Gd_{65}Co_{35}$, and this number along with the calculated values of α and β from the scaling equality [Eq. (2)] are also given in Table II. Similar analyses are done for the other alloys of this work, and the values of γ and δ and the calculated values of α and β are also given in Table II. Deviations from power-law behavior are present at low fields for the critical isotherm as can be seen from Fig. 1(b) for the Gd and Tb alloys of this work. The field below which the critical isotherm shows deviations from a power-law behavior is larger for the Tb alloy than for the Gd alloy.

V. SCALING ANALYSIS OF CRITICAL PHENOMENA

In order to study the critical behavior over a large magnetic-field range and reduced temperature range, we have done a number of scaling analyses. The purpose of doing scaling analyses over progressively smaller reduced temperature ranges is to check as carefully as possible that no deviations from scaling are present at small ϵ, thus giving some confidence that the asymptotic critical

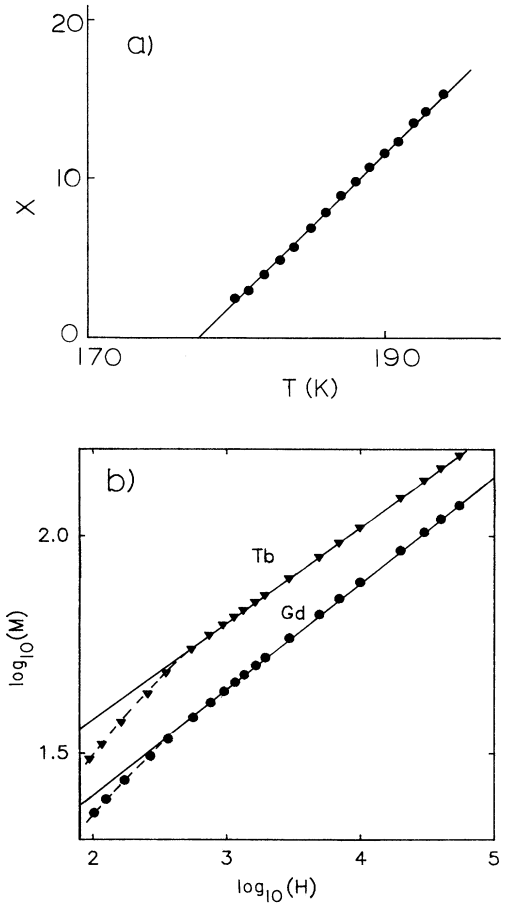

FIG. 1. (a) X [of Eq. (3)] vs T to determine T_c and γ for $Gd_{65}Co_{35}$ and (b) logarithmic plots for the critical isotherm to determine δ for $R_{65}Co_{35}$ where R = Gd and Tb. The solid lines are least-squares fits to the data above 1 kOe. The units of M and H are emu/g and Oe, respectively.

TABLE II. Critical exponents α, β, γ, and δ of this work. A summary of the measured critical exponents for other ferromagnetic rare-earth systems and values predicted by various models is also given. The range of H and ϵ over which good scaling was obtained is also given.

Sample	α	β	γ	δ	T_c (K)	H range (kOe)	ϵ range (10^{-4})	Ref.
Experimental								
$Gd_{65}Co_{35}$	0.08(6)[a]	0.39(1)[a]	1.14(2)	3.95(5)	176.72(4)	0.2–55	0.6–500	This work
$Nd_{50}Co_{50}$	0.05(6)[a]	0.39(1)[a]	1.17(2)	4.00(5)	163.77(5)	0.1–55	1–400	
$Nd_{65}Co_{35}$	0.01(6)[a]	0.39(1)[a]	1.21(3)	4.10(5)	34.99(3)	0.2–55	3–260	
$Tb_{65}Co_{35}$	−0.06(6)[a]	0.38(1)[a]	1.30(2)	4.43(5)	89.10(2)	1.0–55	2–500	
$Gd_{67}Co_{33}$	0.02(7)[a]	0.41(2)	1.16(5)	3.6(1)	169.9(2)	0.2–70	6–400	35
$Gd_{80}Au_{20}$	−0.17(9)[a]	0.44(2)	1.29(5)	3.96(3)	149.5(2)	0.6–70	40–500	36
$Gd_{70}Pd_{30}$	0.32(12)[a]	0.34(2)	1.010(3)	3.95(10)	131.77(20)	0.5–6	60–400	37
c-Gd	0.04(3)[a]	0.381(15)	1.196(3)	3.615(15)	293.3(1)	0.05–10	40–600	38
Theory								
MFT[b]	0.0	0.5	1.0	3.0				20
3D Ising		0.312(5)	1.250(1)	5.00(5)				39
3D Heis.		0.365(3)	1.386(4)	4.80(4)				40

[a]Calculated from measured critical exponents using Eq. (2).
[b]Mean-field theory.

regime is being probed. Using scaling theory, the magnetic equation of state in the critical regime may be written in the reduced form[20]

$$m = f_{\pm}(h) , \tag{4}$$

where

$$m = M/t^{\beta}, \quad h = H/t^{\beta\delta} , \tag{5}$$

where f_+ and f_- are unknown functions of the reduced field h. According to this equation, the magnetization isotherms should collapse onto two separate curves f_+ and f_- corresponding to $T > T_c$ and $T < T_c$ when M and H are plotted in the reduced units of Eq. (5). It should be noted that the critical exponents β and δ are checked over a wide range of temperatures and fields when a scaling analysis is done. In our scaling analyses below, the values of β and δ from Table II are used.

Figure 2(a) shows a scaling plot for $Gd_{65}Co_{35}$ over a reduced temperature range 3×10^{-3}–5×10^{-2} and a magnetic-field range of 0.2–55 kOe. Note that M and H have units of emu/g and Oe, respectively. A good collapse of the magnetic isotherms onto two separate branches is obtained. We also plot the reduced data in logarithmic form in Fig. 2(b) so that the quality of collapse of the isotherms can be seen at small reduced units. This scaling was extended down to progressively smaller reduced temperature ranges, and Fig. 3 shows scaled data over the reduced temperature range closest to T_c, $\epsilon = 6\times10^{-5}$–$9\times10^{-4}$. The data are shown as points in the upper plot in Fig. 3 so that the collapse of the isotherms onto two separate branches may be resolved. Figure 4 shows a scaling plot for all of our data for $Gd_{65}Co_{35}$ in the reduced temperature range 6×10^{-5}–5×10^{-2}. We have also extended our scaling studies to larger values of reduced temperature ($\epsilon = 0.4$) and find that deviations from scaling occur for $\epsilon \geq 0.06$ as a result of the data being outside the critical regime.

We have done a similar study for $Nd_{50}Co_{50}$ where a weak RMA is present. We are able to obtain good ferromagnetic scaling of the magnetic isotherms using the critical exponents β and δ from Table II down to fields of 100 Oe over the reduced temperature range 1×10^{-4}–5×10^{-2}. Figure 5 shows the scaling of the magnetic isotherms over the reduced temperature range closest to T_c for $Nd_{50}Co_{50}$. The data are shown as points as well as symbols so that the collapse of the isotherms onto two separate branches may be resolved more easily.

We next consider $Tb_{65}Co_{35}$, a strong anisotropy system which has a sperimagnetic groundstate. A number of differences are present in the scaling analyses for this system as compared to $Gd_{65}Co_{35}$ and $Nd_{50}Co_{50}$. Figure 6 shows a scaling analysis over a reduced temperature range 6×10^{-3}–5×10^{-2} in linear and logarithmic form. We were only able to scale magnetization isotherms using Eq. (4) above a field H_d of 1000 Oe. Deviations from scaling are illustrated in Fig. 6(b) where the upper plot includes data down to 200 Oe and significant deviations from a collapse of the isotherms onto two branches are evident. This is not due to demagnetization effects since, because of the strong anisotropy, the susceptibility here is small as discussed in Sec. III. We have discussed these deviations in an earlier report,[11] and here we show that these deviations occur for isotherms at reduced temperatures in the 10^{-4} range. Figure 7 shows the scaled magnetic isotherms for the smallest reduced temperature range (down to 2×10^{-4}) represented as symbols (lower plot) and also as points (middle plot). The collapse onto two isotherms can be seen for this (middle) plot. If data below 1000 Oe is added, then strong deviations from scaling are present and this is illustrated in the upper plot where data down to 200 Oe is plotted. All of our data for $Tb_{65}Co_{35}$ (with $H > 1$ kOe) is collected and shown on a scaling plot in Fig. 8. Each branch consists of 20 iso-

therms, and the reduced temperature range is 2×10^{-4}–5×10^{-2}. The values of H_d for the alloys of this work are given in Table I.

Note that the exponent β for $Tb_{65}Co_{35}$ reported here differs from the one reported in Ref. 11 where β was found by varying it over a range of values to obtain the best scaling. We have found that the quality of scaling is somewhat insensitive to β for values in the range 0.40–0.46 for the larger reduced temperatures of Ref. 11 ($1\times10^{-3}<\epsilon<6\times10^{-2}$). Thus we consider the determination of β here where it is calculated from γ and δ using Eq. (2) and then checked by a scaling of the magnetic

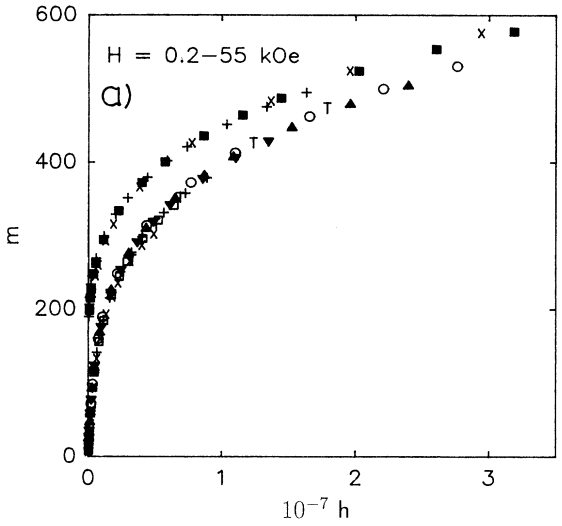

FIG. 2. Ferromagnetic scaling of the magnetic isotherms for $Gd_{65}Co_{35}$ with $\epsilon=3\times10^{-3}$–5×10^{-2}. The data are shown in (a) linear and (b) logarithmic form. The temperatures of the magnetic isotherms are (lower branch) 186.0 K (×), 184.5 K (■), 183.0 K (+), 181.5 K (▼), 180.0 K (▲), 178.5 K (●), 177.0 K (*T*); (upper branch) 175.5 K (×), 174.0 K (■), 172.5 K (+). The units of *M* and *H* are emu/g and Oe, respectively.

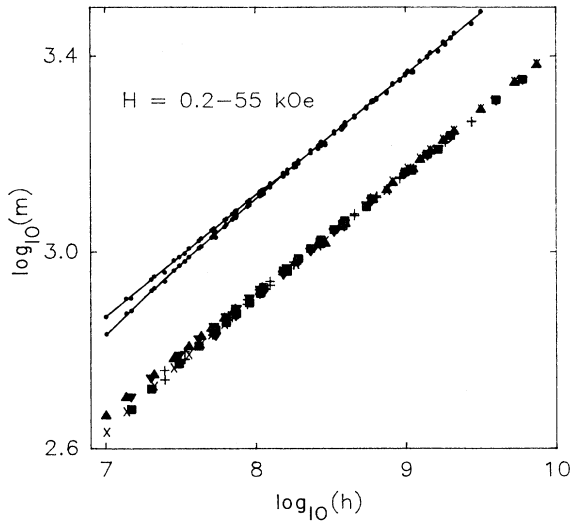

FIG. 3. Ferromagnetic scaling of the magnetic isotherms for $Gd_{65}Co_{35}$ with $\epsilon=6\times10^{-5}$–9×10^{-4}. The temperatures of the magnetic isotherms are (lower branch) 176.90 K (×), 176.86 K (■), 176.82 K (+), 176.78 K (▼), 176.74 K (▲); (upper branch) 176.70 K (×), 176.66 K (■), 176.62 K (+), 176.58 K (▼), 176.54 K (▲). The data are also shifted along the *y* axis and plotted as small single points so that the collapse of the isotherms onto two separate branches may be more clearly seen. The two lines through the shifted data are guides to the eye. The units of *M* and *H* are emu/g and Oe, respectively.

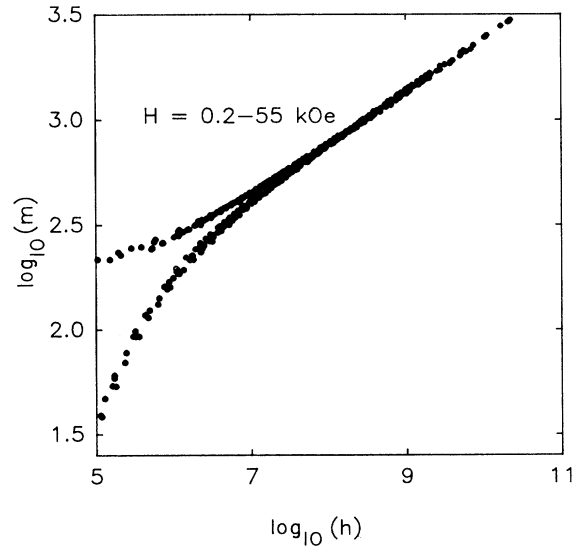

FIG. 4. Scaling of all the magnetic isotherms for $Gd_{65}Co_{35}$ with $\epsilon=6\times10^{-5}$–5×10^{-2}. The lower branch is made up of 22 magnetic isotherms whose temperatures range from 186.00 down to 176.74 K, and the upper branch is made up of 22 isotherms whose temperatures range from 176.70 down to 172.50 K. The units of *M* and *H* are emu/g and Oe, respectively.

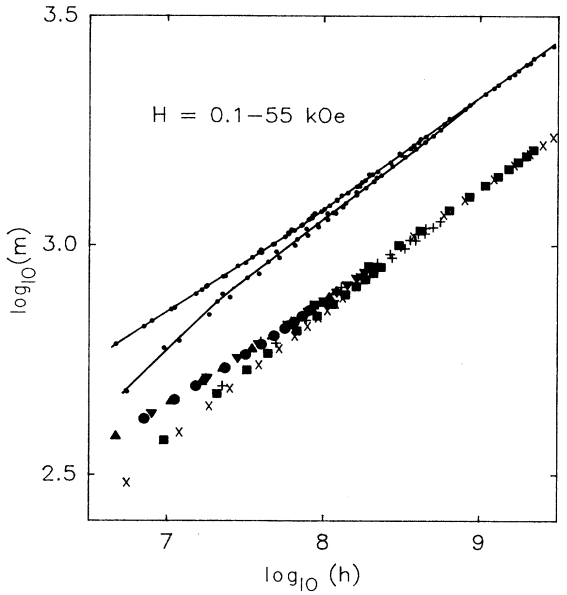

FIG. 5. Ferromagnetic scaling of the magnetic isotherms for $Nd_{50}Co_{50}$ with $\epsilon=1\times10^{-4}$–2×10^{-3}. The temperatures of the magnetic isotherms are (lower branch) 163.90 K (×), 163.85 K (■), 163.80 K (+); (upper branch) 163.75 K (×), 163.70 K (■), 163.65 K (+), 163.60 K (▼), 163.55 K (▲), 163.50 K (●). The data are also shifted along the y axis and plotted as small single points so that the collapse of the isotherms onto two separate branches may be more clearly seen. The two lines through the shifted data are guides to the eye. The units of M and H are emu/g and Oe, respectively.

isotherms using Eq. (5) with reduced temperatures down to 2×10^{-4}, to be more accurate.

Results similar to $Tb_{65}Co_{35}$ were obtained in $Nd_{65}Co_{35}$. Figure 9 shows a scaling plot for the field range 0.5–55 kOe for the magnetic isotherms closest to T_c. The upper plot shows the data as small points so that the collapse may be seen. Inclusion of data below 0.5 kOe (not shown) leads to large deviations from scaling, similar to those seen in $Tb_{65}Co_{35}$ at low fields (below 1000 Oe).

To check the self-consistency of our analysis for the alloys of this work, we have determined the extrapolated spontaneous magnetization (M_s) from a modified Arrott plot. In this plot $M^{1/\beta}$ is plotted against $(H/M)^{1/\gamma}$ as described by Kaul[21] and results in linear isotherms. The intersection of the isotherms with the y axis for $T<T_c$ gives $M_s^{1/\beta}$. A curve fit to Eq. (1b) was done, and the fitted values of β agree within experimental error with those calculated earlier for $Gd_{65}Co_{35}$ and $Nd_{50}Co_{50}$. For $Tb_{65}Co_{35}$ and $Nd_{65}Co_{35}$ where the isotherms did not scale at low fields, we were not able to extrapolate accurately to the y axis and an extrapolated spontaneous magnetization was not determined for these samples.

We have determined the critical amplitudes m_0, h_0/m_0, and B_4 of Eq. (1). Curve fits to the critical isotherm [Eq. 1(d)] were used to determine B_4, and these values are given in Table III. To determine m_0 and h_0/m_0, reduced Arrott plots[21] (m^2 versus h/m) were done. The y intercept gives m_0^2 and the x intercept gives h_0/m_0. Figure 10(a) shows a reduced Arrott plot for $Nd_{50}Co_{50}$, and a similar plot was obtained for $Gd_{65}Co_{35}$. In the case of strong-anisotropy systems ($Nd_{65}Co_{35}$ and $Tb_{65}Co_{35}$) where the scaling did not extend to low fields, we were unable to extrapolate the data with any confidence to the m^2 and h/m axes to determine the intercepts using these plots. Figure 10(b) shows an example

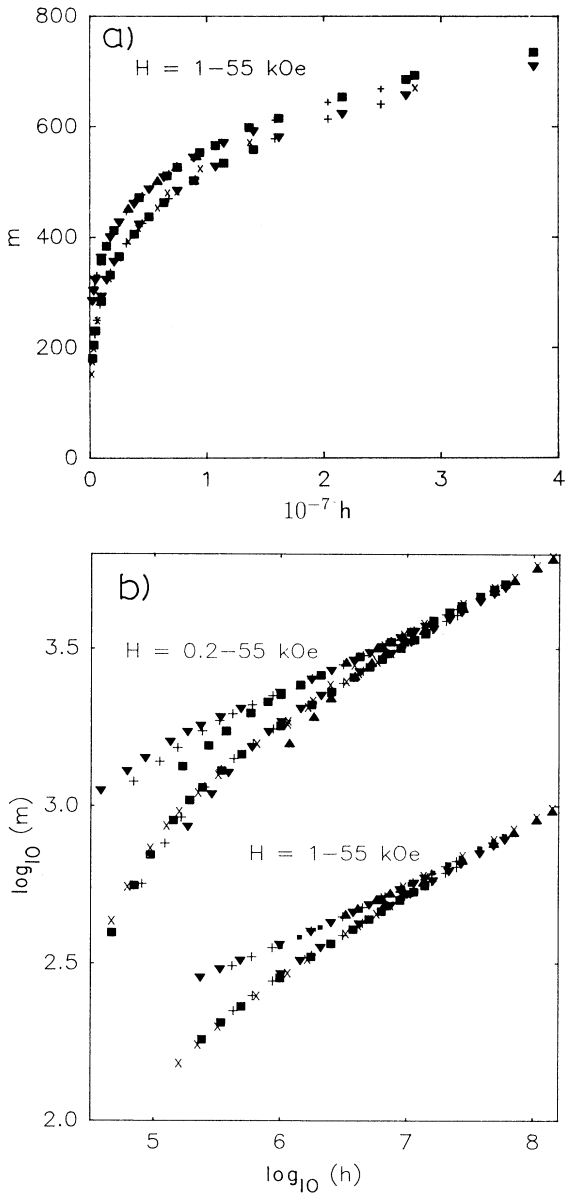

FIG. 6. Ferromagnetic scaling of magnetic isotherms of $Tb_{65}Co_{35}$ with $\epsilon=6\times10^{-3}$–5×10^{-2}. The data is shown in (a) linear and (b) logarithmic form. The temperatures of the magnetic isotherms are (lower branch) 94.00 K (×), 93.00 K (■), 92.00 K (+), 91.00 K (▼), 90.00 K (▲); (upper branch) 89.00 K (×), 88.00 K (■), 87.00 K (+), 86.00 K (▼), 85.00 K (▲). In (b) the data are also plotted down to 0.2 kOe (and shifted along the y axis) to show the deviations from scaling in the latter case. The units of M and H are emu/g and Oe, respectively.

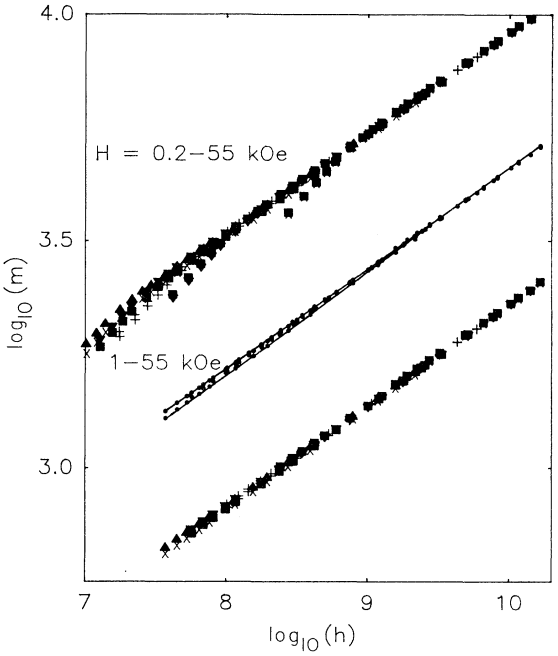

FIG. 7. Ferromagnetic scaling of the magnetic isotherms for $Tb_{65}Co_{35}$ with $\epsilon=2\times10^{-4}$–2×10^{-3}. The temperatures of the magnetic isotherms are (lower branch) 89.28 K (×), 89.24 K (■), 89.20 K (+), 89.16 K (▼), 89.12 K (▲); (upper branch) 89.08 K (×), 89.04 K (■), 89.00 K (+), 88.96 K (▼), 88.92 K (▲). The lower plot shows the data plotted as symbols, and the middle plot shows the data shifted along the y axis and plotted as small single points so that the collapse of the isotherms onto two separate branches may be more clearly seen. The field range for both of these plots is 1–55 kOe. The two lines are guides to the eye. The upper plot (also shifted along the y axis) includes data down to 0.2 kOe to show deviations from scaling. The units of M and H are emu/g and Oe, respectively.

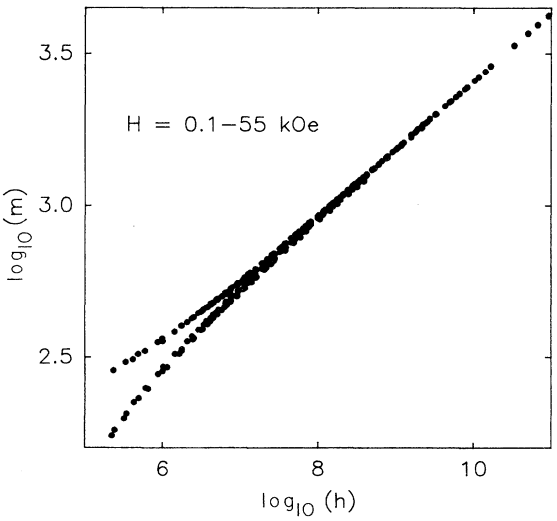

FIG. 8. Scaling of all the magnetic isotherms for $Tb_{65}Co_{35}$ with $\epsilon=2\times10^{-4}$–5×10^{-2}. The lower branch is made up of 20 magnetic isotherms whose temperatures range from 94.00 down to 89.12 K, and the upper branch is made up of 20 isotherms whose temperatures range from 89.08 down to 85.00 K. The units of M and H are emu/g and Oe, respectively.

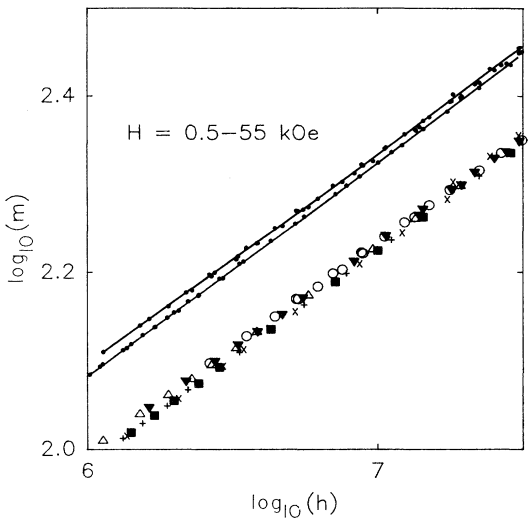

FIG. 9. Ferromagnetic scaling of the magnetic isotherms for $Nd_{65}Co_{35}$ with $\epsilon=3\times10^{-4}$–3×10^{-3}. The temperatures of the magnetic isotherms are (lower branch) 35.08 K (×), 35.06 K (■), 35.04 K (+), 35.02 K (▼), 35.00 K (▲); (upper branch) 34.98 K (×), 34.96 K (■), 34.94 K (+), 34.92 K (▼), 34.90 K (▲). The data are also shifted along the y axis and plotted as single points so that the collapse of the isotherms onto two separate branches may be more clearly seen. The two lines through the shifted data are guides to the eye. The units of M and H are emu/g and Oe, respectively.

for $Tb_{65}Co_{35}$ where the anisotropy is strong. This plot only includes data down to 1 kOe since only data down to this field shows good scaling. We improved the above data analysis and were able to determine the critical amplitudes m_0 and h_0 for these strong-anisotropy alloys using a modified reduced Arrott plot.[21] In this plot, $m^{1/\beta}$ is plotted against $(h/m)^{1/\gamma}$. The data should again collapse onto two separate branches. This plot differs from a reduced Arrott plot in that each branch should be a straight line. A more dependable extrapolation of each branch to the axis may be done with such a plot. Examples are shown for $Nd_{50}Co_{50}$ and $Tb_{65}Co_{35}$ in Fig. 11. The final values of m_0 and h_0/m_0 for all the alloys of this work are taken from such reduced modified Arrott plots and are given in Table III.

Curve fits to the susceptibility for $T>T_c$ [Eq. (2c)] were used to check h_0/m_0 for all the alloys of this work, and these numbers agree within experimental error with those given in Table III. Finally, we have calculated values of the critical amplitude quantities m_0/M_s, $\mu h_0/k_B T_c$, and dm_0^{δ}/h_0 $(d=1/B_4^{\delta})$, and these are also given in Table III. The average magnetic moment per ion, μ, of Table III, used in these calculations was determined by dividing the saturation moment at 4.5 K by the number of ions per unit volume.

VI. DISCUSSION

We have scaled our magnetization data using a ferromagnetic-scaling analysis for a number of alloys with a range of anisotropy strengths. A summary of our

TABLE III. Measured critical amplitudes and their ratios along with some theoretical predictions.

	μ/μ_B	m_0 (emu/g)	h_0/m_0 (10^3)	B_4 (emu/g)	$m_0/M_s(0)$	$\mu h_0/k_B T_c$	dm_0^δ/h_0[a]	Ref.
$Gd_{65}Co_{35}$	4.21(6)	234(5)	3.42(15)	7.20(5)	1.23(6)	1.28(6)	1.1(1)	This Work
$Nd_{50}Co_{50}$	2.13(8)	137(5)	5.11(15)	3.95(5)	1.17(5)	0.58(8)	2.1(2)	
$Nd_{65}Co_{35}$	2.47(8)	47(2)	2.09(8)	2.98(5)	0.42(4)	0.47(3)	0.83(8)	
$Tb_{65}Co_{35}$	5.64(20)	294(10)	0.95(8)	13.9(3)	1.15(6)	1.18(8)	5.7(3)	
$Gd_{67}Co_{33}$	4.74(4)	205.3			0.97(1)	0.665(9)	1.41(10)	35
$Gd_{80}Au_{20}$	5.68(3)	186.0			0.97(1)	0.88(1)	1.46(30)	36
Theory								
MFT					1.73	1.73	1.0	20
3D Ising					1.486	1.52	1.81	39
3D Heisen.					1.69	1.58	1.55	40

results along with critical exponents determined previously for rare-earth alloys, crystalline Gd, and predictions of various models is given in Table II.

It is important to note that the spontaneous magnetization in systems with RMA is expected to be zero below T_c since the order is sperimagnetic or speromagnetic. We have calculated a value of β for these anisotropic systems, but this does not imply that a spontaneous magnetization exists since the scaling does not hold down to low fields. It is simply a parameter used to describe the magnetic properties of the ferromagneticlike state of the system in an applied field.

The critical exponents β and γ for $Gd_{65}Co_{35}$, a system with a very weak RMA, are the same within experimental error as those reported earlier for amorphous $Gd_{67}Co_{33}$, while the value of δ measured here is 9% larger than the value reported earlier.[35] Critical exponents have been reported for two other ferromagnetically ordered Gd systems, $Gd_{80}Au_{20}$ (Ref. 36) and $Gd_{70}Pd_{30}$.[37] Both systems show small differences in at least one critical exponent when compared to those for the $Gd_{65}Co_{35}$ alloy of this work as can be seen from Table II. Critical exponents have also been reported for $(Gd_{72-x}T_x)_{72}Ga_{18}B_{10}$ with T=La,[41] Mn, and Ni,[42] but these systems have strong exchange fluctuations which may modify the values of their critical exponents, and so we will not discuss these systems further here.

In the alloys containing anisotropic rare-earth atoms we observe a systematic increase of the measured critical exponents γ and δ with D/J_0 with $Tb_{65}Co_{35}$, where D/J_0 is the largest, having the largest values of these exponents. The critical exponents α and β remains constant within experimental error. The systematic variation of γ and δ with D/J_0 indicates, most likely, that a crossover is occurring from an isotropic class of system ($Gd_{65}Co_{35}$) where the critical exponents have one set of values to a strong RMA class where the critical exponents γ and δ have modified values. Note that a number of scaling analyses were done at progressively smaller reduced temperatures for each alloy to check that the critical exponents did not vary, thus ensuring that the measurements were made in the critical regime. At large reduced temperatures ($\epsilon > 0.06$), deviations from scaling were observed in all the alloys of this work, indicating the limit of the critical regime.

Critical exponents have also been reported for disordered alloys containing anisotropic rare-earth atoms of the form $(Gd_{1-x}Dy_x)Cu_2$ (Ref. 43) and $(Gd_{1-x}Tb_x)Cu_2$ (Ref. 44) for a number of values of x. The measured critical exponents for these systems differ significantly from those of this work. We note that the anisotropy in these systems is not completely random, as described in Ref. 43, and may explain these differences.

The magnetic isotherms of the alloys of this work also show deviations from scaling at small applied fields. We have quantified the deviations from scaling by determining the field H_d below which deviations from scaling are resolved, and these field values are given in Table I. We have found that demagnetization effects and RMA can contribute to these deviations. $Gd_{65}Co_{35}$ shows a demagnetization limited susceptibility at low fields, and the applied field was corrected for this as described in Sec. III. We believe that deviations from scaling for $Gd_{65}Co_{35}$ below 200 Oe are due to an inadequate demagnetization correction. Similar effects are encountered for other Gd alloys listed in Table II. While a demagnetization correction was applied to the anisotropic samples, it was found to be a small correction even at small applied fields. In these anisotropic alloys, the field below which deviations from scaling were found shows a correlation with the ratio D/J_0 as can be seen from Table I. This is consistent with the observation that the field below which deviations of the critical isotherm from power-law behavior occur has a higher value for the Tb alloy than for the Gd alloy as discussed in Sec. IV. These results suggest that the RMA is responsible for the deviations from scaling at low fields in the Tb- and Nd-based alloys. Indeed, we have shown in separate work that in $Tb_{65}Co_{35}$,[11] where D/J_0 is the largest, the presences of an RMA leads to a spin-glass scaling.

The reduced amplitudes m_0/M_s and dm_0^δ/h_0 for $Gd_{65}Co_{35}$ are close to those reported earlier for $Gd_{67}Co_{33}$. Each of the reduced critical amplitudes (m_0/M_s, $\mu_0 h_0/k_B T_c$, and dm_0^δ/h_0) shows a variation of approximately a factor of 2 for the alloys of this work with no clear systematic dependence on D/J_0. There is also no

clear agreement between the measured amplitudes and those predicted by three-dimensional (3D) models (see Table III).

The critical amplitude ratios for transition-metal systems have been summarized in Table 5 of Ref. 21. Comparison to our results yields some interesting facts. While the amplitude ratios m_0/M_s and dm_0^{δ}/h_0 here are similar to those of crystalline and amorphous transition-metal systems, $\mu_0 h_0/k_B T_c$ shows a large variation in these systems.

The value of $\mu_0 h_0/k_B T_c$ is close to unity for crystalline transition-metal systems, but it is in the range 0.1–0.01 for amorphous transition-metal systems.[21,45] This has been interpreted in terms of a model of transition-metal amorphous alloys in which sort-range magnetic order in the form of large spin patches (moment μ_{eff}) exist at T_c. The existence of these coherent spin clusters is due to the inhomogeneous nature of the amorphous transition-metal alloy.[21,45] The equality $\mu_{\text{eff}} h_0/k_B T_c \cong 1$ gives μ_{eff} and this quantity has been found to be 10–20 times larger than the average atomic moment of an alloy. The question which now arises is, why do the amorphous systems of this work not exhibit large values of μ_{eff}? Two important differences between the alloys of this work and

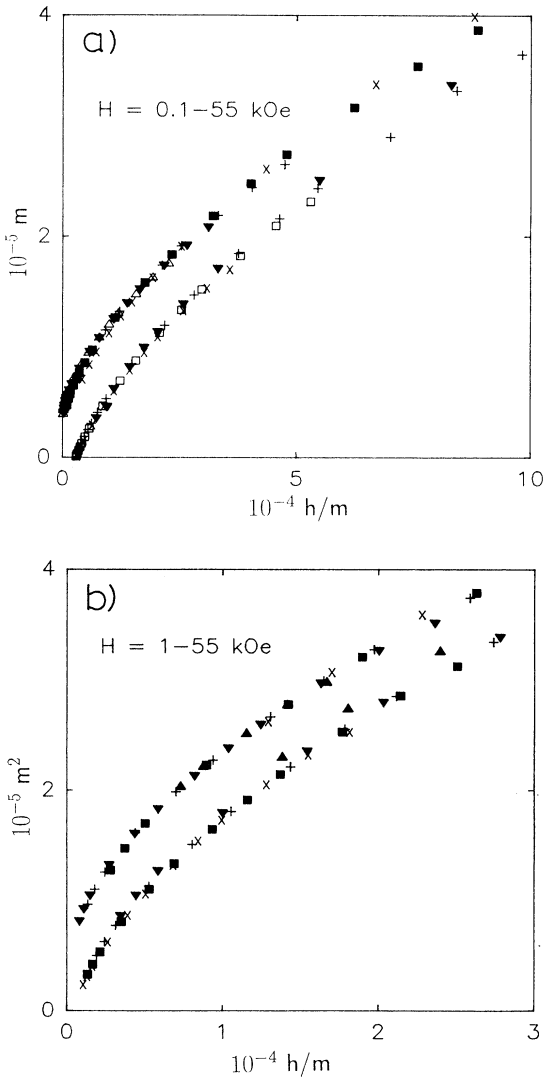

FIG. 10. Reduced Arrott plot for (a) $Nd_{50}Co_{50}$ and (b) $Nd_{65}Nd_{35}$. The isotherms for $Nd_{50}Co_{50}$ cover the range $\epsilon = 4\times10^{-3}$–$4\times10^{-2}$. The temperatures of the magnetic isotherms are (lower branch) 169.00 K (×), 167.50 K (■), 166.00 K (+), 164.50 K (▼); (upper branch) 163.00 K (×), 161.50 K (■), 160.00 K (+), 158.50 K (▼), 157.00 K (▲). The isotherms for $Nd_{65}Co_{35}$ cover the reduced temperature range $\epsilon = 1.4\times10^{-3}$–$2.6\times10^{-2}$. The temperatures of the magnetic isotherms are (lower branch) 35.80 K (×), 35.60 K (■), 35.40, K (+), 35.20 K (▼), 35.00 K (▲); (upper branch 34.80 K (×), 34.60 K (■), 34.40 K (+), 34.20 K (▲), 34.00 K (▲). The units of M and H are emu/g and Oe, respectively.

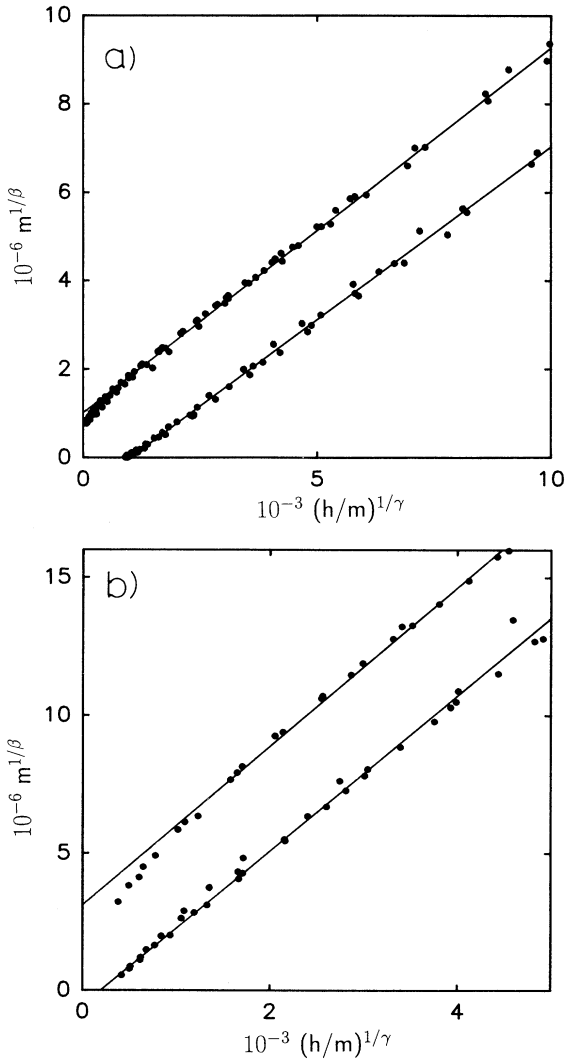

FIG. 11. Reduced modified Arrott plots of magnetic isotherms for (a) $Nd_{50}Co_{50}$ over the field range 0.1–55 kOe and (b) $Tb_{65}Co_{35}$ over the field range 1–55 kOe. Only data at small values of the reduced variables m^2 and h/m are shown. The units of M and H are emu/g and Oe, respectively.

transition-metal amorphous systems are that the exchange is weaker in the alloys of this work than in transition-metal systems and a strong RMA is present in the Tb- and Nd-based alloys of this work. We suggest that this weaker exchange and the presence of RMA both serve to inhibit the formation of coherent spin patches. Thus, in terms of the growth of magnetic order at and below T_c, our systems resemble the elemental crystalline transition-metal systems in that the magnetic order grows from single spins, not coherent clusters.

No theoretical predictions exist concerning a crossover to ferromagnetic critical behavior in finite applied field for a RMA system. The model of Chudnovsky, Saslow, and Serota[4] discussed in Sec. I shows that the magnetic susceptibility is large for a RMA system with weak anisotropy and that a ferromagneticlike phase can appear for a small applied field. This model predicts that the ferromagnetic phase appears above a field which depends on D/J_0, but only applies to low temperatures. Finally, we note the suggestive result of some recent renormalization-group theories discussed above in which the zero-field state below T_c, while being disordered, does possess some characteristics of a ferromagneticlike state. In this quasiferromagnetic state, long-range algebraic order exists in that the ferromagnetic correlation length exhibits a power-law decay rather than an exponential decay.

VII. CONCLUSIONS

We have shown that alloys with strong anisotropy (D/J_0 up to 0.323) show good ferromagnetic scaling over a wide range of reduced temperatures and applied fields.

Crossovers are observed both as a function of applied field and as a function of D/J_0. Below a certain field, whose value increases with D/J_0, deviations from ferromagnetic scaling occur. In separate work we have shown that in the largest D/J_0 alloys[10,11] the magnetization crosses over from a low-field spin-glass scaling regime to a higher-field ferromagnetic scaling regime.

While the crossover as a function of applied field qualitatively resembles the predicted[4] crossover from a correlated speromagnetic state to a finite field state that resembles a ferromagnet, the low-temperature theory of Ref. 4 is not directly applicable to systems close to T_c where our studies have been made. We also note that there are some indications from theory that the magnetic state below T_c in RMA systems has some coherent ferromagneticlike properties in that the correlation length falls off as a power law, a slower decay than exponential.

The critical exponents show a systematic variation with both γ and δ increasing with D/J_0, suggesting a crossover from an isotropic to a random anisotropy class of critical behavior. Also, the calculated values of α and β remain constant within experimental error.

ACKNOWLEDGMENTS

We are grateful to Sy-Huang Liou for allowing us the use of a SQUID magnetometer during part of this work and to David Sellmyer and Kathrin Seibt for useful discussions on critical phenomena.

[1]R. W. Cochrane, R. Harris, and M. J. Zuckermann, Phys. Rep. **48**, 1 (1978).
[2]K. Moorjani and J. M. D. Coey, *Magnetic Glasses* (Elsevier, Amsterdam, 1984).
[3]D. J. Sellmyer and M. J. O'Shea, in *Recent Progress in Random Magnetism,* edited by D. Ryan (World Scientific, Singapore, 1992), p. 71.
[4]E. M. Chudnovksy, W. M. Saslow, and R. A. Serota, Phys. Rev. B **33**, 251 (1986).
[5]M. J. O'Shea and K. M. Lee, Magn. Magn. Mater. **99**, 103 (1991).
[6]J. Filippi, V. S. Amaral, and B. Barbara, Phys. Rev. B **44**, 2842 (1991).
[7]B. Dieny and B. Barbara, Phys. Rev. Lett. **57**, 1169 (1986).
[8]D. J. Sellmyer and S. Nafis, Phys. Rev. Lett. **57**, 1173 (1986).
[9]M. Suzuki, Prog. Theor. Phys. **58**, 1151 (1977).
[10]K. M. Lee, M. J. O'Shea, and D. J. Sellmyer, J. Appl. Phys. **61**, 3616 (1987).
[11]K. M. Lee and M. J. O'Shea, J. Appl. Phys. **67**, 5781 (1990).
[12]R. A. Pelcovits, E. Pytte, and J. Rudnick, Phys. Rev. Lett. **40**, 476 (1978).
[13]A. Aharony and E. Pytte, Phys. Rev. B **27**, 5872 (1983).
[14]S. J. Pickart, J. J. Rhyne, and H. A. Alperin, Phys. Rev. Lett. **33**, 424 (1974); J. J. Rhyne, IEEE Trans. Magn. **MAG-21**, 1990 (1985).
[15]B. Barbara, M. Couach, and B. Dieny, Europhys. Lett. **3**, 1129 (1987).
[16]A. Aharony and E. Pytte, Phys. Rev. B **45**, 1583 (1980).
[17]D. Fisher, Phys. Rev. B **31**, 7233 (1985).
[18]J. Villian and J. F. Fernandez, Z. Phys. B **54**, 139 (1984).
[19]R. Fisch, Phys. Rev. B **39**, 873 (1989); Phys. Rev. Lett. **66**, 2041 (1991).
[20]H. E. Stanley, *Introduction to Phase Transitions and Critical Phenomena* (Oxford University Press, New York, 1971), and references therein.
[21]S. N. Kaul, J. Magn. Mater. **5**, 53 (1985).
[22]A. Kumar, H. R. Krishnamurthy, and E. S. R. Gopal, Phys. Rep. **98**, 57 (1983); M. Vicentini-Missoni, R. I. Joseph, M. S. Green and J. M. H. Levelt, Phys. Rev. B **1**, 2312 (1970).
[23]G. Ahlers, Rev. Mod. Phys. **52**, 489 (1980).
[24]See Table 9 of Ref. 21 and References therein.
[25]M. Fahnle, R. Meyer, and H. Kronmuller, J. Magn. Magn. Mater. **50**, L247 (1985).
[26]M. Fahnle, W.-U Kellner, and H. Kronmuller, Phys. Rev. B **35**, 3640 (1987).
[27]J. Kotzler, J. Magn. Mater. **54-57**, 649 (1986).
[28]*Ferromagnetic Materials* edited by E. P. Wohlfarth (North-Holland, Amsterdam, 1980), Vol. 1, Chap. 1.
[29]*Ferromagnetic Materials,* edited by E. P. Wohlfarth (North-Holland, Amsterdam, 1980), Vol. 1, Chap. 3.
[30]P. Hargraves, R. A. Dunlap, D. J. W. Geldart, and S. P. Ritcey, Phys. Rev. B **38**, 2862 (1988).
[31]M. J. O'Shea, K. M. Lee, and A. Fert, J. Appl. Phys. **67**, 5769 (1990).
[32]M. J. O'Shea, K. M. Lee, and F. Othman, Phys. Rev. B **34**, 4944 (1986).

[33]See Chap. VI of Ref. 2.
[34]K. Fukamichi, T. Goto, T. Sakakibara, S. Todo, K. Aoki, T. Masumoto, J. Magn. Mater. **54**, 239 (1986).
[35]J. Durand, K. Raj, S. J. Poon, and J. I. Budnick, IEEE Trans. Magn. **MAG-14**, 722 (1978).
[36]S. J. Poon and J. Durand, Phys. Rev. B **18**, 6253 (1978).
[37]D. J. Griffiths, D. S. Easton, and D. M. Kroeger, Phys. Rev. B **31**, 287 (1985).
[38]M. N. Deschizeaux and G. Develey, J. Phys. (Paris) **32**, 319 (1971).
[39]*Phase Transitions and Critical Phenomena,* edited by C. Domb and M. S. Green (Academic, New York, 1974), Vol. 3.
[40]L. C. Guillou and J. Zinn-Justin, Phys. Rev. Lett. **39**, 95 (1977); Phys. Rev. B **21**, 3976 (1980).
[41]M. J. O'Shea and D. J. Sellmyer, Phys. Rev. B **32**, 7502 (1985).
[42]J. Jantan and M. J. O'Shea, J. Magn. Magn. Mater. **75**, 175 (1988).
[43]P. M. Gehring, M. B. Salamon, A. del Moral, and J. I. Arnaudas, Phys. Rev. B **41**, 9134 (1990).
[44]J. I. Arnaudas, A. del Moral, P. A. J. de Groot, and C. de la Fuente, J. Magn. Magn. Mater. **104**, 216 (1992).
[45]R. Reisser, M. Seeger, M. Fahnle, and H. Kronmuller, J. Magn. Magn. Mater. **110**, 32 (1992).